



Published in final edited form as:

Nat Neurosci. 2010 December ; 13(12): 1511–1518. doi:10.1038/nn.2684.

TRPV1 activation by endogenous anandamide triggers postsynaptic LTD in dentate gyrus

Andrés E. Chávez, Chiayu Q. Chiu, and Pablo E. Castillo*

Dominick P. Purpura, Department of Neuroscience, Albert Einstein College of Medicine, Kennedy Center, Room 703, Bronx, NY 10461.

Abstract

The transient receptor potential TRPV1 is a nonselective cation channel that mediates pain sensations and is commonly activated by a wide variety of exogenous and endogenous, physical and chemical stimuli. While TRPV1 receptors are mainly found in nociceptive neurons of the peripheral nervous system, these receptors have also been described in the brain where their role is far less understood. Activation of TRPV1 reportedly regulates neurotransmitter release at several central synapses. Here we show, however, that TRPV1 suppresses excitatory transmission in rat and mouse dentate gyrus by regulating *postsynaptic* function in an input-specific manner. This suppression is due to a Ca²⁺-calcineurin and clathrin-dependent internalization of AMPA receptors. Moreover, synaptic activation of TRPV1 triggers a form of long-term depression (TRPV1-LTD) mediated by the endocannabinoid anandamide in a type 1 cannabinoid receptor-independent manner. Thus, our findings reveal a novel form of endocannabinoid- and TRPV1-mediated regulation of synaptic strength at central synapses.

INTRODUCTION

The TRPV1 or Vanilloid VR1 receptor is part of a large family of transient receptor potential (TRP) channels, which typically acts as a molecular detector of noxious signals in primary sensory neurons^{1–2}. This receptor is a homotetrameric, nonselective ligand-gated cation channel that is activated by a wide range of stimuli, including heat, changes in pH, exogenous compounds such as the pungent ingredient in hot chili pepper, as well as endogenous lipid ligands (termed “endovanilloids”) such as anandamide (AEA)³. Though first identified and cloned in peripheral afferent fibers⁴, accumulating evidence indicates that TRPV1 is also expressed in the brain⁵. While the role of TRPV1 in the peripheral nervous system as mediator of noxious stimuli is well established, the function of brain TRPV1 is less understood.

Users may view, print, copy, download and text and data- mine the content in such documents, for the purposes of academic research, subject always to the full Conditions of use: http://www.nature.com/authors/editorial_policies/license.html#terms

*Correspondence should be addressed to: Pablo E. Castillo, M.D., Ph.D., Dominick P. Purpura Department of Neuroscience, Albert Einstein College of Medicine, 1410 Pelham Parkway South, Kennedy Center, Room 703, Bronx, NY 10461, Phone: (718) 430 3263, Fax: (718) 430 8821, pablo.castillo@einstein.yu.edu.

Author contributions: A.E.C., C.Q.C. performed all of the experiments and analyzed the results. A.E.C., C.Q.C. and P.E.C. designed the experiments, interpreted the results and wrote the paper.

The presence of TRPV1 in the brain is supported by diverse experimental approaches, including immunohistochemistry^{6–8}, *in situ* hybridization and reverse transcription-polymerase chain reaction (RT-PCR)^{9–10}, and autoradiography¹¹. These studies reveal that TRPV1 can be found in prefrontal cortex, amygdala, hypothalamus, periaqueductal gray, locus coeruleus, cerebellum, hippocampus and dentate gyrus. Functional studies have demonstrated that exogenous activation of TRPV1 facilitates transmitter release not only in the spinal cord¹² and brainstem¹³ but also in substantia nigra¹⁴, locus coeruleus¹⁵, hypothalamus⁹, and striatum¹⁶. Interestingly, TRPV1 receptors can also mediate a presynaptic form of long-term depression (LTD) at glutamatergic synapses onto CA1 inhibitory interneurons in the hippocampus¹⁷. A similar form of TRPV1-dependent LTD has recently been reported in the developing superior colliculus¹⁸. The precise mechanism by which putative presynaptic TRPV1 receptors can facilitate or suppress transmitter release is unclear. Intriguingly, anatomical evidence suggests that brain TRPV1 can also be found in the postsynaptic compartment^{6,8,19} but its role in synaptic transmission remains elusive. A recent study has shown that TRPV1 receptors mediate some AEA effects in the striatum²⁰. Finally, TRPV1 knockout mice reportedly show deficits in hippocampus-dependent learning²¹, and blockade of TRPV1 receptors in rats suggest that hippocampal TRPV1 activation enables spatial memory retrieval under stressful conditions²².

While all these studies argue for the presence of TRPV1 receptors in the brain, a clear picture of how these receptors regulate neural function, and synaptic transmission in particular, has not yet emerged. To address this issue, we have investigated the role of TRPV1 at excitatory synapses in the dentate gyrus, a brain structure where these receptors are highly expressed^{6,8,10}. Unexpectedly, we found that exogenous activation of TRPV1 receptors reduces synaptic transmission in a transmitter release-independent manner. Moreover, TRPV1 activation by endogenous AEA triggers a form of postsynaptic LTD. These findings not only highlight the diverse mechanisms by which TRPV1 regulates synaptic function but also demonstrate an unconventional way of endocannabinoid signaling in the brain.

RESULTS

TRPV1-mediated depression of excitatory synaptic transmission

To investigate the role of brain TRPV1, we recorded from dentate granular cells (DGCs) and elicited AMPA receptor-mediated excitatory postsynaptic currents (AMPA-EPSCs) by stimulating medial perforant path (MPP) and mossy cell fibers (MCF) in acute hippocampal slices of rat (Supplementary Fig. 1a, see Methods). Pharmacological activation of TRPV1 with the specific agonist capsaicin (CAP) selectively reduced MPP-EPSCs, but not MCF-EPSCs (Fig. 1a), in a dose-dependent manner (Supplementary Fig. 1b), at both 28 and 37°C (Supplementary Fig. 1c). Suppression of MPP-EPSC by 1 μ M CAP was saturating (MPP: 74.2 ± 1.3 % of baseline, $n=10$, $p<0.001$, paired t-test; Fig. 1a, Supplementary Fig. 1b) and was abolished in the presence of 10 μ M capsazepine (CPZ), a specific TRPV1 receptor antagonist (104.1 ± 1.2 % of baseline; $n=6$; $p=0.215$, paired t-test; Fig. 1b, Supplementary Fig. 1b, Supplementary Table 1). CPZ alone had no effect on basal synaptic transmission (Supplementary Fig. 1d). Postsynaptic loading of DGCs with another selective TRPV1

antagonist, AMG9810 (AMG, 3 μ M), also blocked CAP-mediated depression (103.4 ± 1.7 % of baseline; $n=6$; $p=0.196$, paired t-test; Fig. 1b). CAP also mediated an input-specific depression of MPP transmission in mouse dentate gyrus (Supplementary Fig. 1c Supplementary Table 1). In contrast to a recent report²³, CAP-mediated depression was absent in TRPV1 knockout mice (*TRPV1*^{+/+}: 70.0 ± 1.2 % of baseline, $n=7$, $p<0.001$, paired t-test; *TRPV1*^{-/-}: 103.1 ± 4.4 % of baseline, $n=6$, $p=0.560$, paired t-test; Fig. 1c), indicating that in both rat and mouse dentate gyrus TRPV1 activation depresses excitatory synaptic transmission in an input-specific manner. We next investigated the mechanism of this TRPV1-mediated depression.

If TRPV1 activation affected glutamate release^{9,12–18}, CAP would likely depress both AMPAR- and NMDA receptor (NMDAR)-mediated EPSCs to a similar extent. In contrast, we found that CAP had no effect on NMDAR-EPSCs monitored at different holding potentials (-40 mV: 100.9 ± 1.3 % of baseline, $n=5$, $p=0.91$, paired t-test; $+40$ mV: 100.2 ± 3.4 % of baseline, $n=5$, $p=0.93$, paired t-test; Fig. 2a; Supplementary Table 1), suggesting that TRPV1-mediated depression of MPP synaptic transmission is not due to glutamate release modulation. Two additional observations are consistent with this idea. First, CAP-mediated depression of MPP-DGC transmission was not associated with changes in paired pulse ratio (PPR) or coefficient of variation ($1/CV^2$) in both rat and mouse (Supplementary Fig. 1e, Supplementary Table 2). Second, CAP reduced the amplitude but not the frequency of asynchronous MPP-EPSCs evoked in the presence of extracellular strontium (see methods) (Fig. 2b, Supplementary Fig. 1f, Supplementary Table 1), indicating that a reduction in the quantal size, rather than quantal content, likely underlies TRPV1-mediated depression of MPP synaptic transmission.

To directly test whether a postsynaptic modification could account for the TRPV1-mediated depression of transmission, we examined the effects of CAP on DGC responses elicited by brief puffs of glutamate (see Methods), a manipulation that short-cuts transmitter release. The glutamate-evoked responses (monitored at -60 mV) were mediated by AMPARs as indicated by a complete blockade with 10 μ M NBQX (Fig. 2c). Indeed, bath application of 1 μ M CAP depressed glutamate puff-induced responses elicited in the MPP synaptic field (e.g. middle third of the molecular layer), but not in the MCF synaptic field (e.g. inner third of the molecular layer) (MPP: 57.8 ± 4.7 % of baseline, $n=5$, $p<0.001$, paired t-test; MCF: to 100.8 ± 3.0 % of baseline, $n=7$, $p=0.615$, paired t-test; Fig. 2c, Supplementary Table 1). Importantly, CAP-mediated depression of MPP glutamate puff-evoked responses was observed in *TRPV1*^{+/+} but not *TRPV1*^{-/-} mice (*TRPV1*^{+/+}: 63.3 ± 6.6 % of baseline; $n=4$; $p=0.001$, paired t-test; *TRPV1*^{-/-}: 98.2 ± 3.4 % of baseline; $n=4$; $p=0.637$, paired t-test; Fig. 2d, Supplementary Table 1), further supporting a postsynaptic mechanism of action of TRPV1 receptors at MPP-DGC synapses.

If TRPV1 receptors are present on DGCs, one might expect CAP to produce an inward current as previously reported in the peripheral sensory neurons¹, and more recently in the brain¹⁷ (but see²⁰). Intriguingly, we found that bath application of 1 μ M CAP produced a rather weak and variable inward current in DGCs recorded from rat hippocampal slices (14.2 ± 6.1 pA, $n=18$), which was blocked by 10 μ M CPZ or 3 μ M AMG9810 (CPZ: 0.7 ± 1.6 pA, $n=6$; AMG: 1.4 ± 5.1 , $n=6$; Supplementary Fig. 2a). Similar inward current was

observed in *TRPV1*^{+/+} but not *TRPV1*^{-/-} mice (*TRPV1*^{+/+}: 14.8 ± 6.8 pA, n=7; *TRPV1*^{-/-}: 1.0 ± 1.3 , n=6; Supplementary Fig. 2b). TRPV1 receptors are known to desensitize quite rapidly¹. Given the slow CAP perfusion of our slices, some TRPV1 desensitization is expected. To better assess the magnitude of the TRPV1-mediated inward current in DGCs, we recorded from cultured DGCs (see methods) and found that CAP produced a more robust, dose-dependent inward current, which was blocked by 10 μ M CPZ (Supplementary Fig. 2c). Again, similar inward current was observed in *TRPV1*^{+/+} but not *TRPV1*^{-/-} mice (Supplementary Fig. 2d). Together, these results provide additional evidence for functional TRPV1 receptors in DGCs.

TRPV1 receptors mediate a postsynaptic form of long-term depression

TRPV1 receptors have been recently linked to long-term synaptic plasticity in the hippocampus¹⁷ and superior colliculus¹⁸. We therefore tested whether TRPV1 receptor activation could lead to long-lasting depression of synaptic transmission. In fact, the MPP-EPSC depression mediated by a 20-min bath application of 1 μ M CAP could not be fully reversed by subsequent application of 10 μ M CPZ (Fig. 2e, Supplementary Table 1), raising the possibility that transient activation of TRPV1 receptors may trigger a form of long-lasting depression, which becomes independent of TRPV1 activity. This observation prompted us to investigate whether repetitive neural activity, by causing the release of some endogenous TRPV1 ligand(s), might induce a TRPV1-dependent form of long-term depression (LTD) at MPP synapses. To avoid the induction of NMDAR-dependent long-term potentiation (LTP) at MPP synapses²⁴, these experiments were performed in the presence of the NMDAR antagonists d-APV (50 μ M) or MK801 (50 μ M) (note: blockade of NMDARs had no effect on the magnitude of CAP-mediated depression of MPP synaptic transmission; Supplementary Fig. 1g). Under these recording conditions, pairing bursts of presynaptic activity (i.e. MPP repetitive stimulation) with brief postsynaptic depolarizations at 1 Hz (see Methods), induced significant LTD (70.2 ± 4.8 % of baseline, n=10, p<0.001, paired t-test; Fig. 3a, Supplementary Table 3). This depression was abolished in the presence 10 μ M CPZ or 3 μ M AMG (Fig. 3a, Supplementary Table 3; unpaired t-test: Control vs. CPZ, p=0.005; unpaired t-test: Control vs. AMG, p<0.001). This TRPV1-mediated LTD (TRPV1-LTD) was also observed in *TRPV1*^{+/+}, but not *TRPV1*^{-/-} mice (Fig. 3b; unpaired t-test: *TRPV1*^{+/+} vs. *TRPV1*^{-/-}, p<0.001). Consistent with the CAP-mediated depression of MPP transmission (Fig. 1, Supplementary Fig. 1), no significant changes in either PPR or $1/CV^2$ were observed in both rats and mice (Fig. 3a,b, Supplementary Table 2), suggesting that this TRPV1-LTD is expressed postsynaptically.

Like the CAP-mediated depression (Fig. 1a), TRPV1-LTD was also selectively observed at MPP (Fig. 3a,b) but not MCF synapses (Fig. 3c top panel, Supplementary Table 3). TRPV1-LTD induction requires both pre- and postsynaptic activity since presynaptic burst stimulation or postsynaptic depolarizations alone were insufficient to trigger LTD (Supplementary Fig. 3a,b, Supplementary Table 3). In addition, by activating two independent sets of MPP fibers, we found that only those synapses receiving the pairing protocol (i.e. repetitive stimulation and postsynaptic depolarization) expressed TRPV1-LTD, whereas (in the same cell) naïve inputs expressed no plasticity (Fig. 3c bottom panel, Supplementary Table 3). Such input-specificity imposes significant spatial constraints to the

Ca²⁺ rise from multiple sources may be necessary for the induction of TRPV1-LTD. Consistent with this possibility, loading DGCs with the Ca²⁺ chelator BAPTA (20 mM) eliminated both CAP-mediated suppression (99.5 ± 4.9 % of baseline; n=6; p<0.001, unpaired t-test; Fig. 6a) and TRPV1-LTD (106.8 ± 7.3 % of baseline; n=6; p<0.001, unpaired t-test; Fig. 6b). In addition, depletion of intracellular Ca²⁺ stores by including 30 μM cyclopiazonic acid (CPA) in the bath, a manipulation that has no effect on basal synaptic transmission (Supplementary Fig. 4), significantly reduced CAP-mediated depression of MPP-EPSC (87.0 ± 1.9 % of baseline; n=10; p<0.001, unpaired t-test; Fig. 6a) and abolished TRPV1-LTD (98.8 ± 1.4 % of baseline; n=7; p<0.001, unpaired t-test; Fig. 6b).

Given the requirement of postsynaptic Ca²⁺ rise in CAP-mediated suppression and TRPV1-LTD, we next explored whether the Ca²⁺/calmodulin-dependent protein phosphatase calcineurin (CaN, or protein phosphatase 2B/PP2B), a Ca²⁺-dependent effector mediating different forms of LTD whose expression mechanism relies on postsynaptic AMPAR removal^{26–28}, could also underlie TRPV1-LTD. We found that two different CaN inhibitors, 50 μM FK506 or 25 μM Cyclosporin A (CyA), which did not affect basal synaptic transmission (Supplementary Fig. 4), completely blocked both CAP-mediated depression and TRPV1-LTD (Fig. 6c,d, Supplementary Table 4). As CaN forms a molecular complex with the GTPase dynamin²⁹, which is required for clathrin-dependent AMPAR endocytosis³⁰, we investigated the role of dynamin-dependent endocytosis of AMPARs in TRPV1-LTD. Indeed, postsynaptic loading of 50 μM dynamin inhibitory peptide (DIP) abolished both CAP-suppression and TRPV1-LTD (Fig. 6e,f, Supplementary Table 4). Postsynaptic loading of a DIP scrambled peptide (50 μM) had no effect on TRPV1-LTD (Fig. 6f, Supplementary Table 4). Together, these findings suggest that activation of TRPV1 receptors leads to a Ca²⁺/CaN- and dynamin-dependent internalization of AMPARs.

The endocannabinoid anandamide mediates TRPV1-LTD

TRPV1 receptors can be activated by various lipid ligands, including the endocannabinoid/endovanilloid anandamide (AEA)^{31–33}. Since AEA is known to be released upon demand in a Ca²⁺ dependent manner^{34–35}, we hypothesized that TRPV1-LTD could be triggered by endogenous AEA that is likely produced following repetitive activation of MPP glutamatergic fibers. To test this possibility, we first examined whether exogenous application of AEA could modulate MPP synaptic transmission in a TRPV1-dependent manner. Bath application of 30 μM AEA in the presence of the FAAH inhibitor URB597 (1 μM) to block AEA degradation, and the type 1 cannabinoid receptor (CB1R) antagonist AM251 (4 μM), significantly suppressed MPP-EPSC amplitude (69.1 ± 3.1 % of baseline; n=6; p<0.001, paired t-test; Fig. 7a, Supplementary Table 5). Blocking FAAH activity with URB597 had no effect on synaptic transmission (Supplementary Fig. 5, Supplementary Table 5). Like the CAP-mediated depression of MPP-EPSCs (Fig. 1), this AEA-mediated depression was input-specific as indicated by the lack of change of MCF-EPSCs (Fig. 7a, Supplementary Table 5), and was not associated with changes in PPR (baseline: 0.80 ± 0.02, AEA: 0.79 ± 0.04, n=6, p=0.856, paired t-test; Fig. 7a) or 1/CV² (baseline: 11.4 ± 1.1; AEA: 11.6 ± 1.5; n=6; p=0.821, paired t-test; Fig. 7a). Similarly, loading DGCs with 30 μM AEA also depressed MPP-EPSCs, while PPR and 1/CV² remained unchanged (Fig. 7b, Supplementary Table 2). Importantly, this depression was insensitive to AM251, but was

completely abolished by CPZ (Fig. 7b, Supplementary Table 5), indicating that AEA modulates MPP synaptic transmission in a TRPV1-dependent but CB1R-independent manner. Consistent with these results, the CB1R agonist WIN55,212-2 (5 μ M) did not affect MPP-EPSCs at naïve synapses (Supplementary Fig. 6). Furthermore, bath application of AEA also depressed MPP-EPSC in *CB1R*^{-/-} but not in *TRPV1*^{-/-} mice (*CB1R*^{-/-}: 74.1 \pm 1.4 % of baseline; n=8; p<0.001, paired t-test; *TRPV1*^{-/-}: 96.5 \pm 3.7 % of baseline; n=7; p=0.323, paired t-test; Fig. 7c, Supplementary Table 5). Together, these results strongly suggest that AEA-mediated depression of synaptic transmission is likely mediated via TRPV1 receptors.

To directly explore whether endogenous AEA could mediate TRPV1-LTD, we delivered a sub-threshold induction protocol, which by itself did not induce any form of synaptic plasticity (Fig. 8a), and tested whether such a protocol could induce LTD under conditions of reduced AEA degradation with 1 μ M URB597. Indeed, under these recording conditions the sub-threshold induction protocol triggered robust LTD (to 69.1 \pm 5.1 % of baseline; n=8; p<0.001, paired t-test; Fig. 8a), which could not be induced in the presence of CPZ (to 100.0 \pm 1.2 % of baseline; n=7; p=0.321, paired t-test; Fig. 8a). This LTD (i.e., elicited in the presence of URB597) was also observed in *TRPV1*^{+/+} but not in *TRPV1*^{-/-} mice (Fig. 8b, Supplementary Table 5), supporting the notion that the effects of URB597 are likely mediated by AEA specifically targeting TRPV1 receptors. Finally, given that TRPV1 receptors could be modulated by the endocannabinoid 2-AG36, the other major endocannabinoid besides AEA, and that our LTD induction protocol likely mobilizes 2-AG37, we examined the potential contribution of 2-AG in TRPV1-LTD. To this end, we used the diacylglycerol (DAG) lipase inhibitor tetrahydrolipstatin (THL), which is known to block 2-AG synthesis and endocannabinoid-dependent LTD at hippocampal inhibitory synapses (e.g., I-LTD)³⁷. However, we found that TRPV1-LTD was normally induced in DGCs loaded with 4 μ M THL (Fig. 8c top panel, Supplementary Table 4), whereas in interleaved experiments THL blocked I-LTD (Fig. 8c bottom panel, Supplementary Table 4). Together, these results suggest that endogenous AEA, but not 2-AG, is likely released upon neural activity to regulate MPP-DG synaptic transmission and trigger TRPV1-LTD.

DISCUSSION

We have identified a previously unknown function of TRPV1 in the central nervous system. Our results indicate that TRPV1 receptors, in addition to modulating presynaptic release, as extensively reported in several brain structures^{9,12–18}, can also reduce synaptic transmission by promoting AMPAR endocytosis. Moreover, we show that TRPV1 receptors can selectively modulate transmission in an input-specific and long-lasting manner. Finally, we show that the endocannabinoid AEA mediates TRPV1-LTD independently of CB1R activation, thereby highlighting a novel form of endocannabinoid signaling in the brain. A summary of the underlying mechanisms of TRPV1-LTD can be found in Supplementary Fig. 7.

In the last ten years, endocannabinoids have become the most prominent example of retrograde signaling molecules in the CNS^{38–40}. Typically, endocannabinoids move backward across the synapse and bind presynaptic CB1Rs to reduce transmitter release

Author Manuscript

Author Manuscript

Author Manuscript

either in a transient or long-lasting manner. Our study supports the notion that in addition to this conventional intercellular form of signaling, endocannabinoids can also act intracellularly, not only by targeting CB1Rs to reduce neuronal intrinsic excitability⁴¹, but also by targeting TRPV1 receptors to selectively suppress AMPAR-mediated synaptic transmission. Brain TRPV1 receptors have been recently identified as mediators of a *presynaptic* form of LTD at excitatory inputs onto hippocampal inhibitory interneurons¹⁷. In contrast, we show that TRPV1 receptors can mediate a *postsynaptic* form of LTD at excitatory inputs onto DGCs. Of note, a virtually identical postsynaptically expressed TRPV1-LTD has been recently identified in the nucleus accumbens by Malenka and co-workers (Grueter et al., submitted), indicating that this form of plasticity is likely to be a widespread phenomenon in the brain. TRPV1 receptors have been reported in DGCs⁶ and, consistent with these anatomical studies, our results now provide evidence for functional TRPV1 receptors in these cells. Importantly, TRPV1 modulation of synaptic transmission is input-specific, a property that could arise from the selective expression of TRPV1 receptors at some synapses (e.g. MPP) but not others (e.g. MCF), as well as differential TRPV1 functional properties across synapses. In this context, it is worth mentioning that in contrast to TRPV1 receptors, CB1Rs regulate synaptic transmission selectively at MCF synapses but not MPP (Supplementary Fig. 6) or lateral perforant path⁴² synapses. The significance of this synaptic specificity and specialization of endocannabinoid signaling to the function of the dentate gyrus warrants further investigation.

Author Manuscript

Author Manuscript

There is strong evidence in support of AEA as a modulator/activator of TRPV1 receptors in both the peripheral and central nervous system^{3,43}. Consistent with our findings that AEA modulates synaptic function in the dentate gyrus, key anabolic and catabolic enzymes for this endogenous ligand have been found in DGCs of the mouse brain¹⁹. Our results argue that AEA, but not 2-AG, modulates synaptic transmission via TRPV1. While AEA can be tonically released to homeostatically regulate inhibitory transmission via CB1Rs⁴⁴, we have found no evidence for AEA tone on TRPV1 receptors (Supplementary Fig. 5). Rather, AEA is produced upon activity within DGCs and most likely remains in the intracellular space to act locally in a synapse-specific manner. As a result, AEA selectively opens postsynaptic TRPV1 channels near active but not inactive synapses. Notably, TRPV1 are known to be promiscuous receptors that can be activated and modulated by a wide range of compounds^{1,43,45–46}. Thus, while our study identifies AEA as a mediator of TRPV1-LTD, other endogenous TRPV1 ligands could also participate in a TRPV1-mediated regulation of synaptic transmission. Particularly relevant among these compounds are other unsaturated N-acylethanolamines (NAEs), 12-(S)-lipoxygenase (12-LOX) products of arachidonic acid, and unsaturated N-acyldopamines (NADAs)^{43,45}. Future studies will have to address the role and relative contribution of these various endogenous ligands in regulating synaptic transmission via TRPV1 receptors.

Author Manuscript

In addition to TRPV1, induction of TRPV1-LTD requires postsynaptic calcium rise and mGluR5 activation. Our results suggest that multiple calcium sources (e.g. calcium influx via L-type VGCCs and TRPV1 receptors, calcium release from internal stores) participate in plasticity, but the relative contribution of these sources remains to be determined. The fact that CAP triggers a modest and highly-variable TRPV1-dependent inward current in DGCs

(Supplementary Fig. 2) contrasts with the relatively robust and reliable CAP-mediated suppression of MPP synaptic transmission, suggesting that some other TRPV1-mediated step could be involved. As recently proposed²⁰, TRPV1 channels could reside in intracellular organelles, a possibility supported by immunohistochemical studies showing intracellular TRPV1 in DGCs⁶. Finally, our results show that activation of mGluR5 is necessary but not sufficient to induce TRPV1-LTD. Previous studies have shown functional coupling between TRPV1 and mGluR5 in nociceptive neurons, and such TRPV1-mGluR5 coupling may underlie sensitization to nociceptive stimuli^{47–48}. Further, TRPV1 receptors could be directly activated by DAG generated downstream mGluR5 activation⁴⁸, raising the possibility that DAG could also mediate mGluR5 actions in DGCs, and perhaps interact with AEA synergistically to induce plasticity.

TRPV1 receptors have recently emerged as novel targets for alternative therapeutic strategies (for a recent review, see⁴⁹). While such strategies rely on the notion that TRPV1 are selectively expressed in the peripheral nervous system where they mediate pain sensations^{1,4}, our findings not only reinforces the notion that functional TRPV1 receptors may regulate transmission and plasticity at central synapses, but also show that the role of brain TRPV1 receptors is more diverse than current data suggests.

METHODS

Hippocampal slice preparation

Acute transverse hippocampal slices (400 μm thick) were prepared from Wistar rats, postnatal day 15 (P15) to P32, and C57BL/6 mice (*TRPV1*^{+/+}/*TRPV1*^{-/-}: P18–P32; *CB1R*^{+/+}/*CB1R*^{-/-}: P24–P34). Animal handling and use followed a protocol approved by the Animal Care and Use Committee of Albert Einstein College of Medicine, in accordance with National Institutes of Health guidelines. Briefly, the hippocampi were isolated and cut using a DTK-2000 vibrating microslicer (Dosaka EM Co., Ltd.) in a solution containing (in mM): 215 sucrose, 2.5 KCl, 26 NaHCO₃, 1.6 NaH₂PO₄, 1 CaCl₂, 4 MgCl₂, 4 MgSO₄ and 20 glucose. Thirty minutes post sectioning, the cutting medium was gradually switched to extracellular artificial cerebrospinal (ACSF) recording solution containing: 124 NaCl, 2.5 KCl, 26 NaHCO₃, 1 NaH₂PO₄, 2.5 CaCl₂, 1.3 MgSO₄ and 10 glucose. All solutions were equilibrated with 95% O₂ and 5% CO₂ (pH 7.4). Slices were incubated for at least 30 min in the ACSF solution prior to recordings.

Electrophysiology

All experiments, except where indicated, were performed at $28 \pm 1^\circ\text{C}$ in a submersion-type recording chamber perfused at $\sim 1\text{--}2$ ml/min with ACSF supplemented with the GABA-A receptor antagonist picrotoxin (100 μM). Whole-cell patch-clamp recordings using a Multiclamp 700A amplifier (Molecular Devices) were made from DGCs voltage clamped at -60 mV (unless otherwise stated) using patch-type pipette electrodes ($\sim 3\text{--}4$ M Ω) containing (in mM): 131 Cs-Gluconate, 8 NaCl, 1 CaCl₂, 10 EGTA, 10 glucose, 10 HEPES; pH 7.2, 285 mmol/kg. For intracellular loading of the calcium chelator BAPTA (Fig. 6a,b), 20 mM Cs-Gluconate, 10 mM EGTA and 1 mM CaCl₂ were replaced with 20 mM BAPTA (osmolarity and pH was adjusted with CsOH). For strontium experiments (Fig. 2b),

extracellular CaCl_2 was removed and 8 mM SrCl_2 and 1 mM EGTA was added to the ACSF (pH was adjusted with NaOH). Series resistance ($\sim 14\text{--}28\text{ M}\Omega$) was monitored throughout all experiments with a -5 mV , 80 ms voltage step, and cells that exhibited significant change in series resistance ($>20\%$) were excluded from analysis. To stimulate excitatory synaptic inputs, two monopolar stimulating patch-type pipettes were filled with ACSF and placed in the supragranular layer (SGL; $<40\text{ }\mu\text{m}$ from the cell body layer) to activate MCF inputs and in the middle third of the molecular layer to stimulate MPP inputs. MPP-DGC synapses were activated at low stimulus intensity (2–5 V, 200 μs square-wave pulses), whereas MCF-inputs were activated at a higher stimulus intensity (7–19 V, 200 μs square-wave pulses). To verify the identity of synaptic inputs in the dentate gyrus, 1 μM DCG-IV, which selectively reduces MPP but not MCF synaptic transmission⁴², was routinely applied at the end of experiments (e.g., Fig. 1a). In some experiments (Fig. 2c,d), exogenous puff application of L-glutamate (1 mM, 25–30 ms, 1–2 PSI) was applied using a Picospritzer III (Parker Instruments) connected to a patch pipette (resistance, $\sim 3\text{--}4\text{ M}\Omega$). The tip of the puffer pipette was positioned within the MPP or MCF synaptic field in the molecular layer. Glutamate-evoked responses were elicited in the presence of 100 μM picrotoxin while voltage holding DGCs at -60 mV . Both LTD and LTP experiments and analyses in *TRPV1*^{+/+} and *TRPV1*^{-/-} mice were done in a blind fashion.

Paired-pulse ratio (PPR) was defined as the ratio of the amplitude of the second EPSC to the amplitude of the first EPSC. The coefficient of variation ($1/\text{CV}^2$) was calculated as the squared mean EPSC amplitude divided by EPSC variance. Both PPR and $1/\text{CV}^2$ were calculated 10 min before and 15 to 20 min after pharmacological activation of TRPV1 receptors or application of TRPV1-LTD induction protocol. TRPV1-LTD in the rat was evoked using a pairing protocol consisting of a series of 4 stimuli (100 Hz) paired with a small postsynaptic depolarization (30 mV for 30 ms), repeated 600 times at 1 Hz. In the mouse, a slightly modified protocol was required: 2 stimuli (70 ms interval) paired with small postsynaptic depolarization (30 mV for 30 ms) repeated 900 times at 1 Hz. For I-LTD experiments (Fig. 8c), IPSCs were recorded from CA1 pyramidal cells voltage-clamped at $+10\text{ mV}$ in ACSF containing 10 μM NBQX and 25 μM d-APV to block AMPA/kainate and NMDA receptors, respectively. I-LTD was induced after 10 min of stable baseline by theta-burst stimulation (TBS), which consisted of a series of 10 bursts of 5 stimuli (100 Hz within the burst, 200 ms interburst interval) repeated 4 times (5 s apart). The magnitude of I-LTD was compared 25–30 min after TBS protocol in the absence or presence of intracellular loading of the DGL inhibitor THL.

Pharmacological agents were bath applied after establishment of a stable baseline ($\sim 10\text{--}15$ min), and their effects were measured after responses reached a new steady state (typically >15 min). Cells that exhibited significant rundown ($>10\%$ within the first 10 min) before drug application were discarded. Drugs were obtained from Sigma, Tocris and Ascent Scientific, except URB597 that was acquired from Cayman Chemical (Ann Arbor, MI). Stock solutions were prepared in DMSO (Picrotoxin, CAP, CPZ, AMG9810, URB597, FK506, CPA, WIN, AM251) or ethanol (AEA) and added to the ACSF as needed. Total DMSO or ethanol in the ACSF was maintained at $<0.1\%$ and 0.2% , respectively. Excitatory postsynaptic currents (EPSCs) were elicited at 20 s intervals, filtered at 2.2 kHz, and

acquired at 5 kHz using a custom-made software written in Igor Pro 4.09A (Wavemetrics, Inc., Lake Oswego, OR, USA).

Dentate granule cell cultures

For recordings in cultured DGCs (Supplementary Fig. 2), both rat and mouse dentate gyrus were isolated from postnatal day 0 (P0), and DGCs were cultured as described elsewhere⁵⁰. Experiments were performed on cultures from P14 to P17 days *in vitro* in the presence of 0.5 μ M TTX to block action potential generation, and 10 μ M NBQX, 100 μ M picrotoxin, 4 μ M MPEP, 100 μ M LY367385 and 3 μ M CGP 55845 to block excitatory and inhibitory synaptic transmission.

Statistical analysis

Statistical comparisons were made using unpaired and paired two-tailed Student's t-test at the $p < 0.05$ significance level in OriginPro 7.0 software (OriginLab Corporation, Northampton, MA). Cumulative probability plots of asynchronous MPP-EPSCs were compared using the Kolmogorov-Smirnov (K-S) test. Unless otherwise indicated, all values are provided as the mean \pm s.e.m. and illustrated traces are averages of 31–40 responses.

Supplementary Material

Refer to Web version on PubMed Central for supplementary material.

Acknowledgments

This work was supported by NIH grants to PEC (DA017392, MH081935). AEC was partially supported by a Ruth L Kirschstein Award (F32 NS071821). We thank all members of Castillo Lab for comments on the manuscript and Drs. Barry Connors and Scott Nawy for kindly providing *TRPV1*^{-/-} mice, and Drs. Reed Carroll and Alma Rodenas-Ruano for providing DGC cultures.

References

1. Caterina MJ, Julius D. The vanilloid receptor: a molecular gateway to the pain pathway. *Annu Rev Neurosci.* 2001; 24:487–517. [PubMed: 11283319]
2. Ramsey IS, Delling M, Clapham DE. An introduction to TRP channels. *Annu Rev Physiol.* 2006; 68:619–647. [PubMed: 16460286]
3. Ross RA. Anandamide and vanilloid TRPV1 receptors. *Br J Pharmacol.* 2003; 140:790–801. [PubMed: 14517174]
4. Caterina MJ, et al. The capsaicin receptor: a heat-activated ion channel in the pain pathway. *Nature.* 1997; 389:816–824. [PubMed: 9349813]
5. Kauer JA, Gibson HE. Hot flash: TRPV channels in the brain. *Trends Neurosci.* 2009; 32:215–224. [PubMed: 19285736]
6. Cristino L, et al. Immunohistochemical localization of cannabinoid type 1 and vanilloid transient receptor potential vanilloid type 1 receptors in the mouse brain. *Neuroscience.* 2006; 139:1405–1415. [PubMed: 16603318]
7. Sanchez JF, Krause JE, Cortright DN. The distribution and regulation of vanilloid receptor VR1 and VR1 5' splice variant RNA expression in rat. *Neuroscience.* 2001; 107:373–381. [PubMed: 11718993]
8. Toth A, et al. Expression and distribution of vanilloid receptor 1 (TRPV1) in the adult rat brain. *Brain Res Mol Brain Res.* 2005; 135:162–168. [PubMed: 15857679]

9. Sasamura T, Sasaki M, Tohda C, Kuraishi Y. Existence of capsaicin-sensitive glutamatergic terminals in rat hypothalamus. *Neuroreport*. 1998; 9:2045–2048. [PubMed: 9674591]
10. Mezey E, et al. Distribution of mRNA for vanilloid receptor subtype 1 (VR1), and VR1-like immunoreactivity, in the central nervous system of the rat and human. *Proc Natl Acad Sci U S A*. 2000; 97:3655–3660. [PubMed: 10725386]
11. Roberts JC, Davis JB, Benham CD. [³H]Resiniferatoxin autoradiography in the CNS of wild-type and TRPV1 null mice defines TRPV1 (VR-1) protein distribution. *Brain Res*. 2004; 995:176–183. [PubMed: 14672807]
12. Yang K, Kumamoto E, Furue H, Yoshimura M. Capsaicin facilitates excitatory but not inhibitory synaptic transmission in substantia gelatinosa of the rat spinal cord. *Neurosci Lett*. 1998; 255:135–138. [PubMed: 9832191]
13. Doyle MW, Bailey TW, Jin YH, Andresen MC. Vanilloid receptors presynaptically modulate cranial visceral afferent synaptic transmission in nucleus tractus solitarius. *J Neurosci*. 2002; 22:8222–8229. [PubMed: 12223576]
14. Marinelli S, et al. Presynaptic facilitation of glutamatergic synapses to dopaminergic neurons of the rat substantia nigra by endogenous stimulation of vanilloid receptors. *J Neurosci*. 2003; 23:3136–3144. [PubMed: 12716921]
15. Marinelli S, Vaughan CW, Christie MJ, Connor M. Capsaicin activation of glutamatergic synaptic transmission in the rat locus coeruleus in vitro. *J Physiol*. 2002; 543:531–540. [PubMed: 12205187]
16. Musella A, et al. TRPV1 channels facilitate glutamate transmission in the striatum. *Mol Cell Neurosci*. 2009; 40:89–97. [PubMed: 18930149]
17. Gibson HE, Edwards JG, Page RS, Van Hook MJ, Kauer JA. TRPV1 channels mediate long-term depression at synapses on hippocampal interneurons. *Neuron*. 2008; 57:746–759. [PubMed: 18341994]
18. Maione S, et al. TRPV1 channels control synaptic plasticity in the developing superior colliculus. *J Physiol*. 2009; 587:2521–2535. [PubMed: 19406878]
19. Cristino L, et al. Immunohistochemical localization of anabolic and catabolic enzymes for anandamide and other putative endovanilloids in the hippocampus and cerebellar cortex of the mouse brain. *Neuroscience*. 2008; 151:955–968. [PubMed: 18248904]
20. Maccarrone M, et al. Anandamide inhibits metabolism and physiological actions of 2-arachidonoylglycerol in the striatum. *Nat Neurosci*. 2008; 11:152–159. [PubMed: 18204441]
21. Marsch R, et al. Reduced anxiety, conditioned fear, and hippocampal long-term potentiation in transient receptor potential vanilloid type 1 receptor-deficient mice. *J Neurosci*. 2007; 27:832–839. [PubMed: 17251423]
22. Li HB, et al. Antistress effect of TRPV1 channel on synaptic plasticity and spatial memory. *Biol Psychiatry*. 2008; 64:286–292. [PubMed: 18405883]
23. Benninger F, Freund TF, Hajos N. Control of excitatory synaptic transmission by capsaicin is unaltered in TRPV1 vanilloid receptor knockout mice. *Neurochem Int*. 2008; 52:89–94. [PubMed: 17651868]
24. Errington ML, Lynch MA, Bliss TV. Long-term potentiation in the dentate gyrus: induction and increased glutamate release are blocked by D(-)aminophosphonovalerate. *Neuroscience*. 1987; 20:279–284. [PubMed: 2882444]
25. Fagni L, Chavis P, Ango F, Bockaert J. Complex interactions between mGluRs, intracellular Ca²⁺ stores and ion channels in neurons. *Trends Neurosci*. 2000; 23:80–88. [PubMed: 10652549]
26. Malenka RC, Bear MF. LTP and LTD: an embarrassment of riches. *Neuron*. 2004; 44:5–21. [PubMed: 15450156]
27. Mulkey RM, Endo S, Shenolikar S, Malenka RC. Involvement of a calcineurin/inhibitor-1 phosphatase cascade in hippocampal long-term depression. *Nature*. 1994; 369:486–488. [PubMed: 7515479]
28. Winder DG, Sweatt JD. Roles of serine/threonine phosphatases in hippocampal synaptic plasticity. *Nat Rev Neurosci*. 2001; 2:461–474. [PubMed: 11433371]
29. Lai MM, et al. The calcineurin-dynamin 1 complex as a calcium sensor for synaptic vesicle endocytosis. *J Biol Chem*. 1999; 274:25963–25966. [PubMed: 10473536]

30. Carroll RC, et al. Dynamin-dependent endocytosis of ionotropic glutamate receptors. *Proc Natl Acad Sci U S A*. 1999; 96:14112–14117. [PubMed: 10570207]
31. Smart D, et al. The endogenous lipid anandamide is a full agonist at the human vanilloid receptor (hVR1). *Br J Pharmacol*. 2000; 129:227–230. [PubMed: 10694225]
32. van der Stelt M, et al. Anandamide acts as an intracellular messenger amplifying Ca²⁺ influx via TRPV1 channels. *Embo J*. 2005; 24:3026–3037. [PubMed: 16107881]
33. Zygmunt PM, et al. Vanilloid receptors on sensory nerves mediate the vasodilator action of anandamide. *Nature*. 1999; 400:452–457. [PubMed: 10440374]
34. Di Marzo V, et al. Formation and inactivation of endogenous cannabinoid anandamide in central neurons. *Nature*. 1994; 372:686–691. [PubMed: 7990962]
35. Piomelli D. The molecular logic of endocannabinoid signalling. *Nat Rev Neurosci*. 2003; 4:873–884. [PubMed: 14595399]
36. Golech SA, et al. Human brain endothelium: coexpression and function of vanilloid and endocannabinoid receptors. *Brain Res Mol Brain Res*. 2004; 132:87–92. [PubMed: 15548432]
37. Chevaleyre V, Castillo PE. Heterosynaptic LTD of hippocampal GABAergic synapses: a novel role of endocannabinoids in regulating excitability. *Neuron*. 2003; 38:461–472. [PubMed: 12741992]
38. Chevaleyre V, Takahashi KA, Castillo PE. Endocannabinoid-mediated synaptic plasticity in the CNS. *Annu Rev Neurosci*. 2006; 29:37–76. [PubMed: 16776579]
39. Kano M, Ohno-Shosaku T, Hashimoto-dani Y, Uchigashima M, Watanabe M. Endocannabinoid-mediated control of synaptic transmission. *Physiol Rev*. 2009; 89:309–380. [PubMed: 19126760]
40. Regehr WG, Carey MR, Best AR. Activity-dependent regulation of synapses by retrograde messengers. *Neuron*. 2009; 63:154–170. [PubMed: 19640475]
41. Bacci A, Huguenard JR, Prince DA. Long-lasting self-inhibition of neocortical interneurons mediated by endocannabinoids. *Nature*. 2004; 431:312–316. [PubMed: 15372034]
42. Chiu CQ, Castillo PE. Input-specific plasticity at excitatory synapses mediated by endocannabinoids in the dentate gyrus. *Neuropharmacology*. 2008; 54:68–78. [PubMed: 17706254]
43. Starowicz K, Nigam S, Di Marzo V. Biochemistry and pharmacology of endovanilloids. *Pharmacol Ther*. 2007; 114:13–33. [PubMed: 17349697]
44. Kim J, Alger BE. Reduction in endocannabinoid tone is a homeostatic mechanism for specific inhibitory synapses. *Nat Neurosci*. 2010; 13:592–600. [PubMed: 20348918]
45. Pingle SC, Matta JA, Ahern GP. Capsaicin receptor: TRPV1 a promiscuous TRP channel. *Handb Exp Pharmacol*. 2007:155–171. [PubMed: 17217056]
46. Tominaga M, et al. The cloned capsaicin receptor integrates multiple pain-producing stimuli. *Neuron*. 1998; 21:531–543. [PubMed: 9768840]
47. Hu HJ, Bhave G, Gereau RWt. Prostaglandin and protein kinase A-dependent modulation of vanilloid receptor function by metabotropic glutamate receptor 5: potential mechanism for thermal hyperalgesia. *J Neurosci*. 2002; 22:7444–7452. [PubMed: 12196566]
48. Kim YH, et al. Membrane-delimited coupling of TRPV1 and mGluR5 on presynaptic terminals of nociceptive neurons. *J Neurosci*. 2009; 29:10000–10009. [PubMed: 19675234]
49. Wong GY, Gavva NR. Therapeutic potential of vanilloid receptor TRPV1 agonists and antagonists as analgesics: Recent advances and setbacks. *Brain Res Rev*. 2009; 60:267–277. [PubMed: 19150372]
50. Marsden KC, Beattie JB, Friedenthal J, Carroll RC. NMDA receptor activation potentiates inhibitory transmission through GABA receptor-associated protein-dependent exocytosis of GABA(A) receptors. *J Neurosci*. 2007; 27:14326–14337. [PubMed: 18160640]

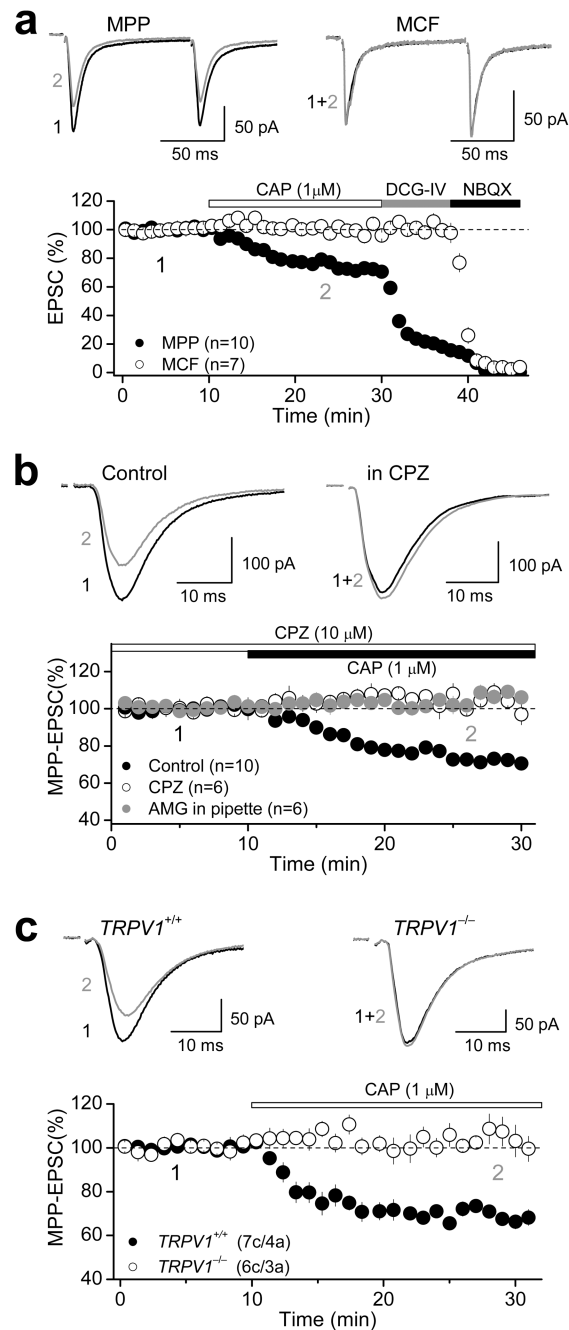


Figure 1. Functional evidence for TRPV1 receptors in the dentate gyrus

a, Pharmacological activation of TRPV1 receptors with the agonist capsaicin (CAP, 1 μM) depresses AMPAR-EPSC in an input-specific manner. *Top panel*: Representative traces of two consecutive AMPAR-EPSCs (100 ms interstimulus interval) before (*black*) and after (*gray*) bath application of 1 μM CAP at both medial perforant path (MPP) and mossy cell fibers (MCF). *Bottom panel*: Summary plot showing the effect of CAP on AMPAR-EPSC. Application of the group II mGluR agonist DCG-IV (1 μM) selectively depressed MPP- but not MCF-EPSCs, and subsequent application of the AMPAR antagonist NBQX (10 μM)

abolished the remaining DCG-IV insensitive component. **b**, Average traces (*top panel*) and summary data (*bottom panel*) showing that pre-treatment with the TRPV1 antagonist capsazepine (CPZ, 10 μ M) or loading of DGCs with the antagonist AMG9830 (AMG, 3 μ M) eliminates CAP-mediated depression of AMPAR-EPSC in the MPP. **c**, CAP-mediated depression of AMPAR-EPSC is also present in *TRPV1*^{+/+} but not *TRPV1*^{-/-} mice. In all panels, averaged sample traces taken at times indicated by numbers are shown next to each summary plot. Number of cells (c) and animals (a) are indicated in parentheses. Summary data consist of mean \pm s.e.m.

Author Manuscript

Author Manuscript

Author Manuscript

Author Manuscript

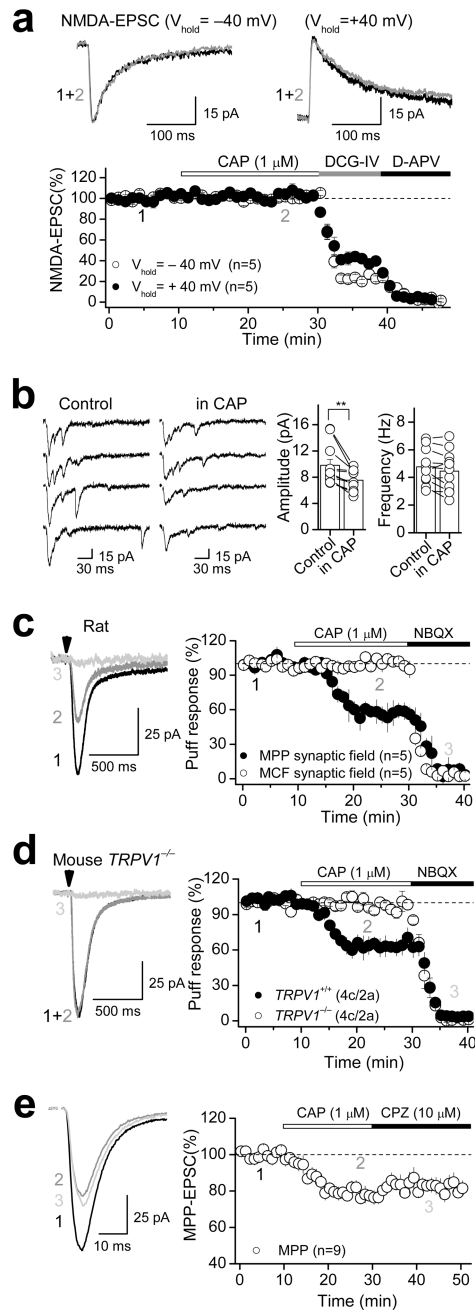


Figure 2. Postsynaptic TRPV1-mediated suppression of excitatory transmission

a, CAP exerted no effect on NMDAR-mediated transmission measured at -40 mV and $+40 \text{ mV}$ in the presence of $10 \mu\text{M}$ NBQX. **b**, Representative traces (*left*) and summary plot (*right*) showing that $1 \mu\text{M}$ CAP only depresses the amplitude but not the frequency of asynchronous AMPA-EPSC. $** p < 0.01$. **c**, CAP selectively depressed AMPAR-mediated responses evoked by puffing 1 mM glutamate in the MPP but not the MCF synaptic field in rat. Representative responses evoked in the MPP synaptic field before (*black*) and after CAP (*gray*) application are shown on the left. Vertical arrowheads indicate the time of glutamate

puffs. NBQX completely abolished glutamate puff-evoked EPSCs (light gray), indicating that the responses were mediated by AMPARs. Summarized time course of CAP-mediated effect is shown on the right. **d**, Representative traces (*left*) and summary plot (*right*) showing that CAP also mediated depression of AMPAR-mediated responses evoked by puffing glutamate in *TRPV1*^{+/+} but not in *TRPV1*^{-/-} mice. **e**, Representative traces (*left*) and summary plot (*right*) showing that transient pharmacological activation of TRPV1 receptors triggers long-lasting depression of AMPAR-mediated transmission that cannot be rescued by subsequent application of the TRPV1 antagonist CPZ. In all panels, averaged sample traces taken at times indicated by numbers are shown next to each summary plot. Number of cells (c) and animals (a) are indicated in parentheses. Summary data consist of mean ± s.e.m.

Author Manuscript

Author Manuscript

Author Manuscript

Author Manuscript

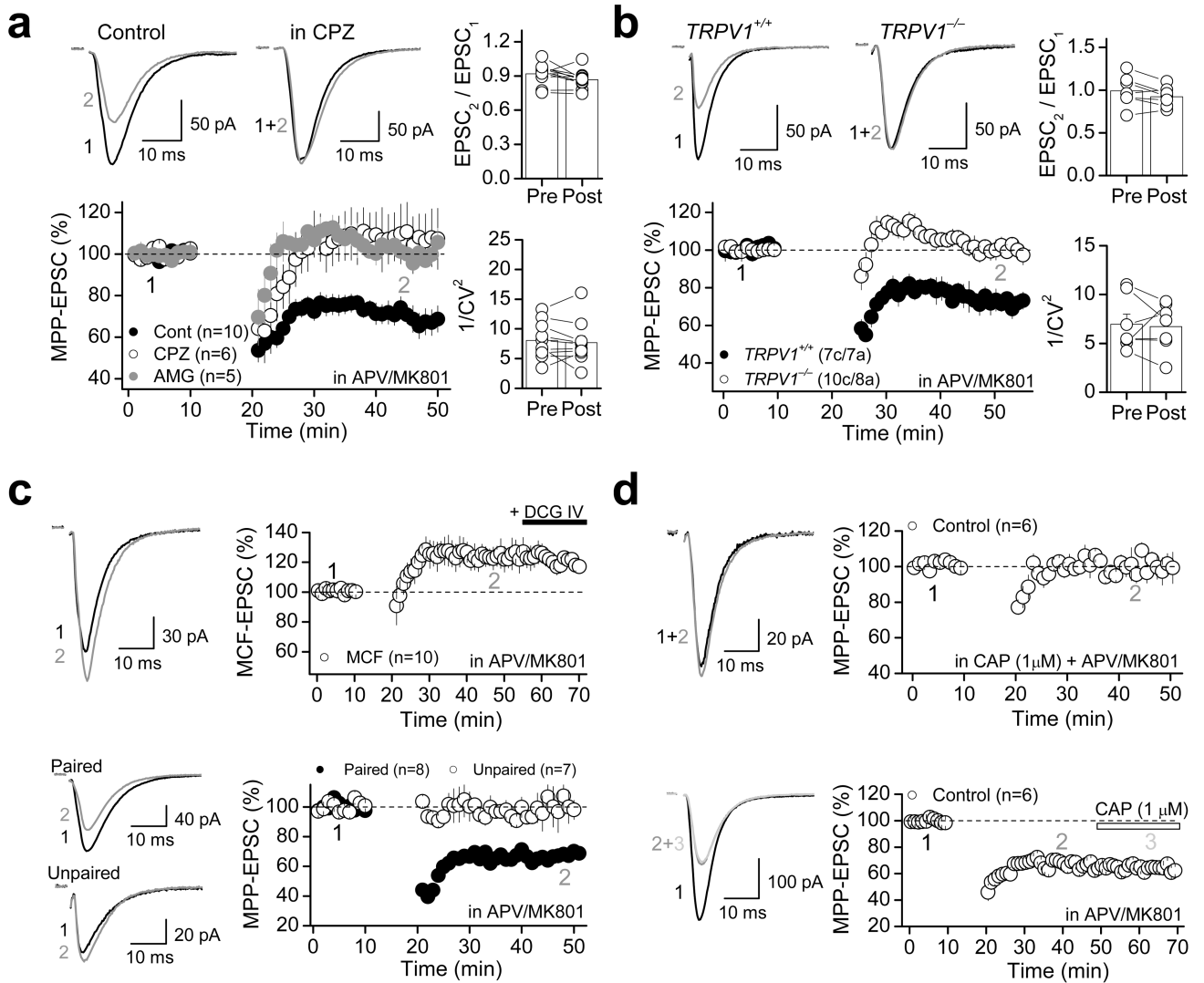


Figure 3. TRPV1-mediated long-term depression at MPP-DGC synapses

a, In the presence of the NMDAR antagonists d-APV (50 μM) or MK-801 (50 μM), 1 Hz-pairing protocol (see Methods) induced a robust LTD in rat dentate gyrus, which is blocked by the antagonists CPZ (10 μM) or AMG (3 μM). No significant changes in either PPR (*right top*) and $1/CV^2$ (*right bottom*) were observed before (pre) and after (post) LTD induction. **b**, The 1 Hz pairing protocol induced robust LTD in *TRPV1*^{+/+} but not *TRPV1*^{-/-} mice. As seen in rat, TRPV1-LTD in mice was not associated with changes in PPR (*right top*) or $1/CV^2$ (*right bottom*). **c**, 1 Hz pairing protocol delivered to MCF inputs did not trigger LTD, strongly suggesting that TRPV1-LTD is input-specific (*top panel*). TRPV1-LTD also shows associativity (i.e., only MPP synapses whose activation was paired with depolarization underwent depression) and specificity (i.e., LTD did not spread to unpaired MPP synapses; *bottom panel*). **d**, TRPV1-LTD could not be induced in the presence of 1 μM CAP (*top panel*), while CAP had no effect after TRPV1-LTD was established (*bottom panel*). **c–d**, Representative responses evoked before (*black*) and after 1 Hz protocol (*gray*)

are shown on the left. Summarized time course are shown on the right. Number of cells (c) and animals (a) are indicated in parentheses. Summary data consist of mean \pm s.e.m.

Author Manuscript

Author Manuscript

Author Manuscript

Author Manuscript

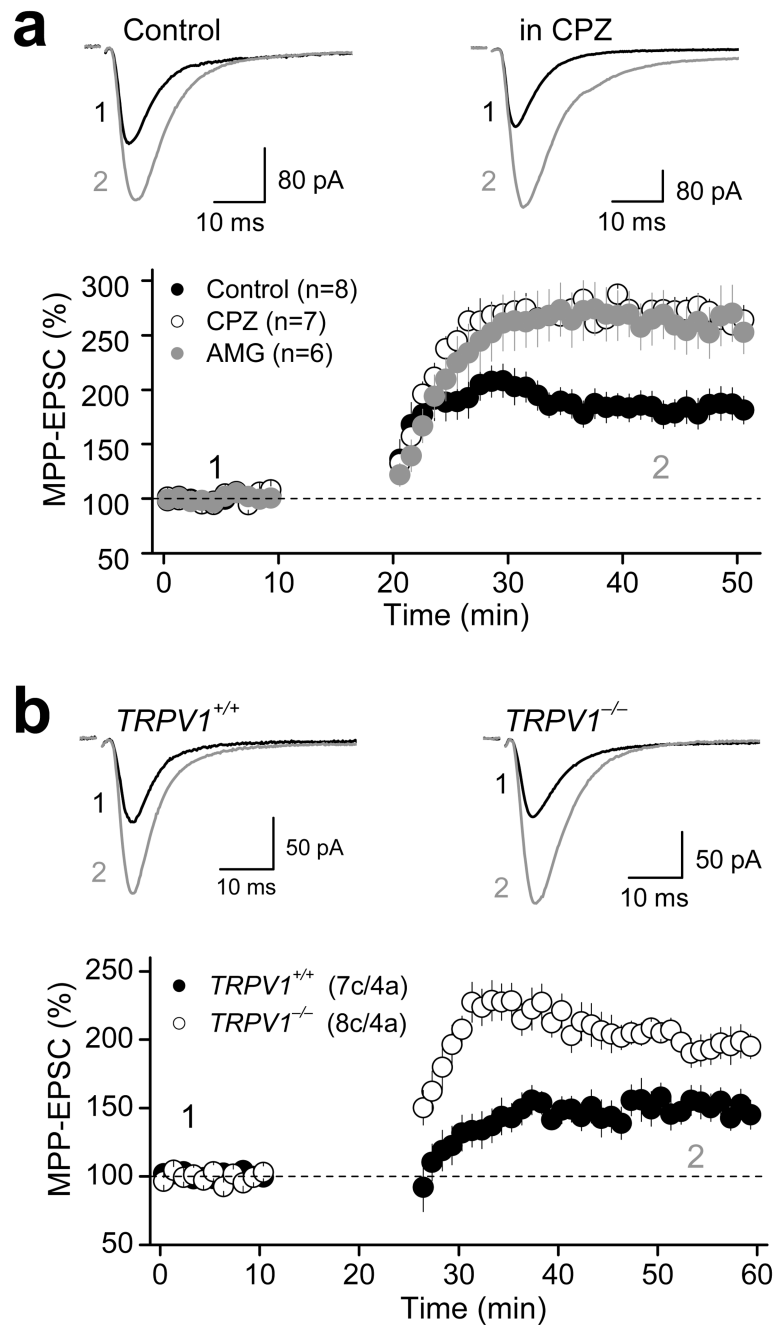


Figure 4. Role of TRPV1 receptors in long-term potentiation at MPP-DGC synapses

a, Under more physiological recording conditions (i.e. intact NMDAR transmission), a 1 Hz pairing protocol induced robust MPP-LTP, whose magnitude is enhanced in the presence of CPZ (10 μ M) or AMG (3 μ M) in the bath. *Top*: Average traces before (black) and after (gray) LTP induction. *Bottom*: Summary plot showing the enhancement of LTP in the presence of CPZ or AMG. **b**, LTP is also enhanced in $TRPV1^{-/-}$ mice compared to $TRPV1^{+/+}$ mice. Number of cells (c) and animals (a) are indicated in parentheses. Summary data consist of mean \pm s.e.m.

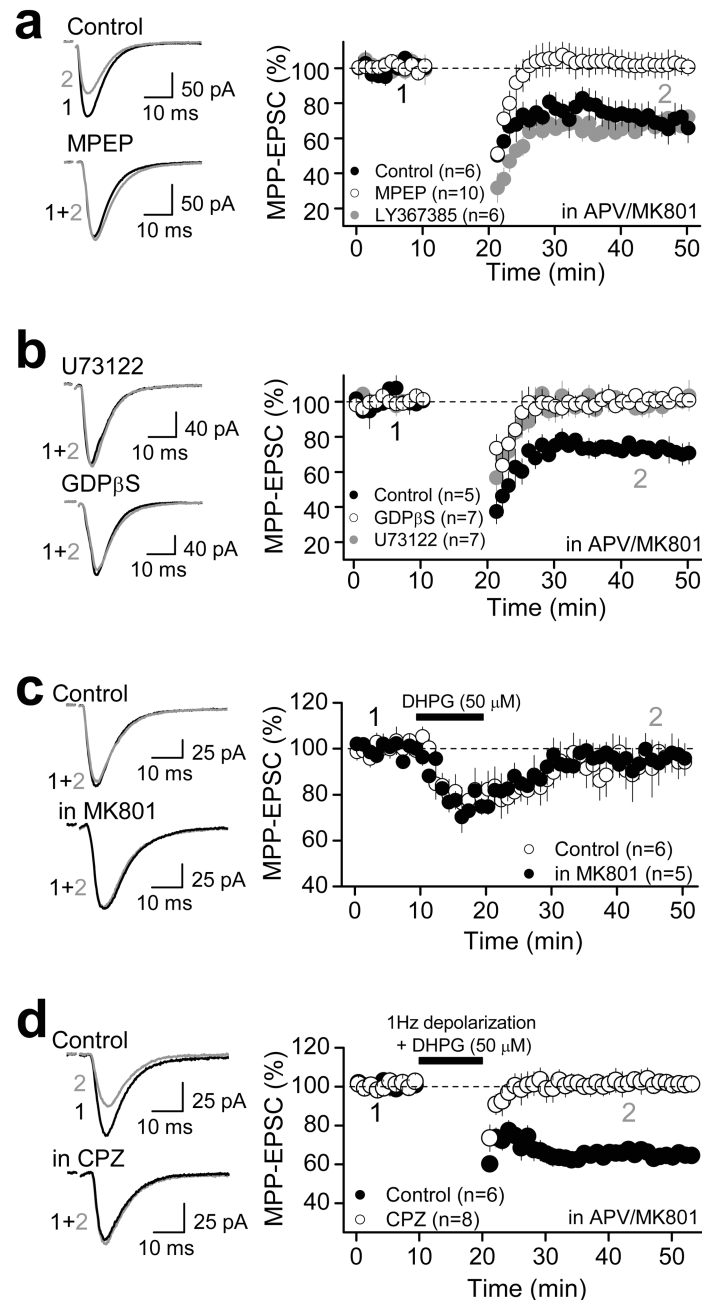


Figure 5. Activation of mGluR5 is necessary but not sufficient to induce TRPV1-LTD
a, TRPV1-LTD was blocked by bath application of 4 μ M MPEP but not by 100 μ M LY367385, suggesting that activation of mGluR5, but not mGluR1 is required for TRPV1-LTD induction. **b**, Loading DGCs with the G-protein antagonist GDP β S (1 mM) or the PLC blocker U73122 (5 μ M) blocked TRPV1-LTD, suggesting the involvement of G-protein and downstream signaling via phospholipase C (PLC) in the induction of TRPV1-LTD. **c**, Group I mGluR activation with DHPG (50 μ M) for 10 min was not sufficient to trigger long-lasting depression of MPP synaptic transmission in the absence or in the presence of the NMDAR

antagonist MK801 (50 μ M). **d**, DHPG (50 μ M) paired with depolarization triggered robust TRPV1-LTD at MPP-DGC synapses, which was blocked by CPZ (10 μ M). **a–d**, Averaged EPSCs before (black) and 25 min after LTD induction (gray) are shown on the left side. Summary plots (mean \pm s.e.m.) showing the time course and drug effects on TRPV1-LTD are shown on the right.

Author Manuscript

Author Manuscript

Author Manuscript

Author Manuscript

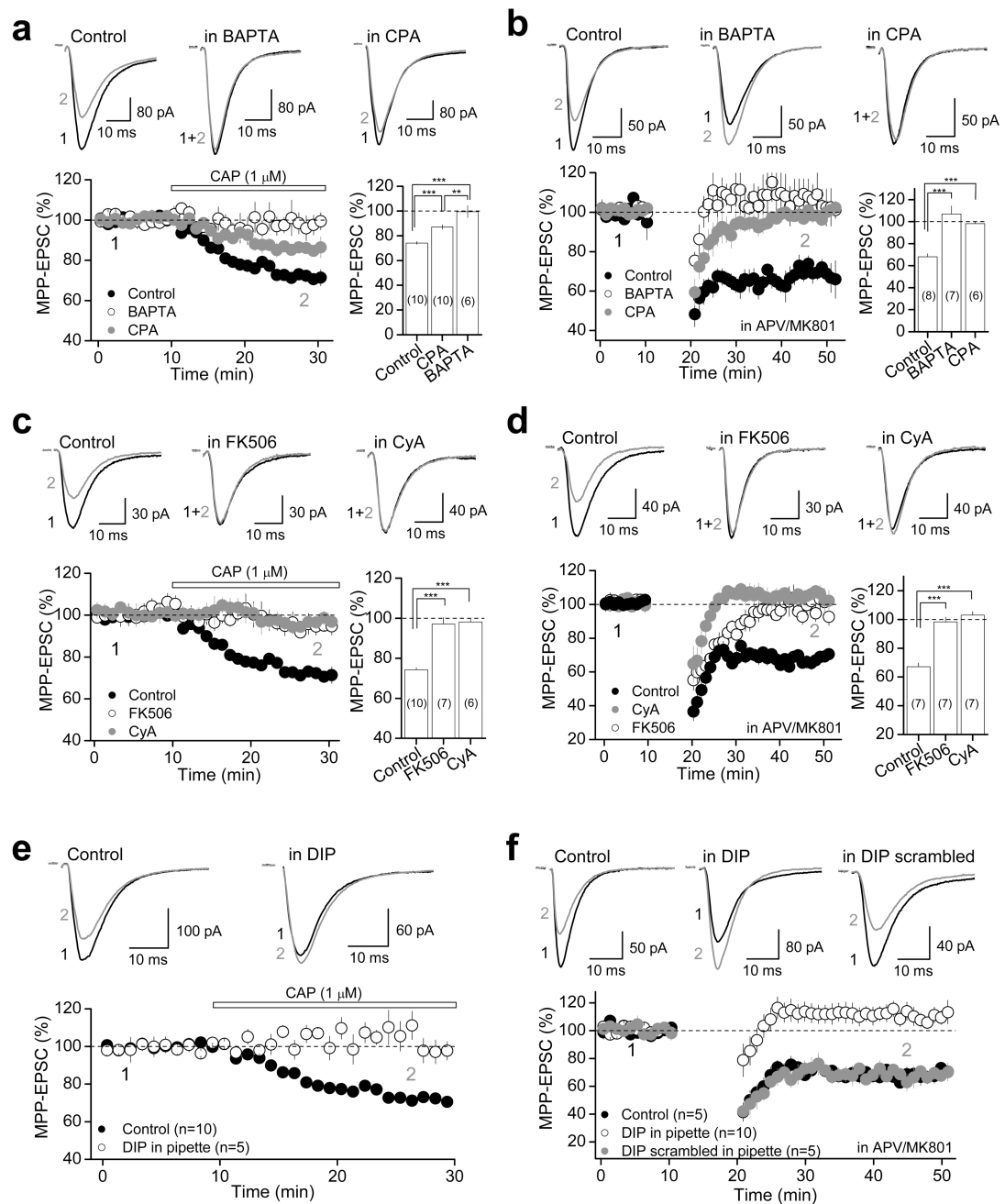


Figure 6. Molecular mechanism underlying TRPV1-mediated depression of synaptic transmission

a and **b**, Both CAP-mediated depression and TRPV1-LTD require Ca^{2+} rise and Ca^{2+} release from internal stores. *Top*, representative averaged traces under control conditions (*left*), in DGCs loaded with 20 mM BAPTA (*center*) and in hippocampal slices treated with 30 μ M CPA (*right*); *bottom*, summary data. Bar plots show MPP-EPSC amplitude changes calculated 15–20 min following application of CAP (**a**) or 25–30 min following LTD induction protocol (**b**). **c** and **d**, Representative averaged traces (*top*) and summary plots

(*bottom*) showing that two different calcineurin inhibitors FK506 (50 μ M) and Cyclosporin A (CyA; 25 μ M) blocked both CAP-mediated depression (**c**) and TRPV1-LTD (**d**). **e** and **f**: Intracellular loading of the dynamin inhibitory peptide (DIP, 50 μ M) abolished both CAP-mediated depression (**e**) and TRPV1-LTD (**f**). Loading DGCs with a scrambled DIP (50 μ M) did not affect TRPV1-LTD (**f**). **a–d**, The number of cells is indicated in parenthesis and asterisks represent significance: *** $p < 0.001$, ** $p < 0.01$. All summary data consist of mean \pm s.e.m.

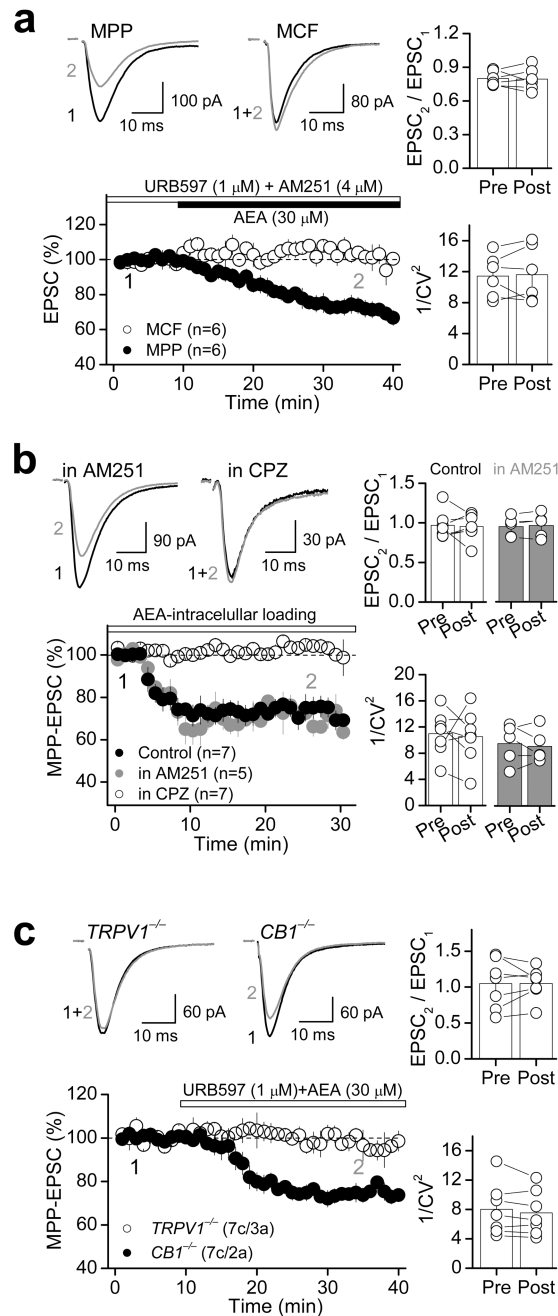


Figure 7. The endocannabinoid anandamide (AEA) suppresses excitatory synaptic transmission via TRPV1 receptors

a. Representative averaged traces (*top left*) and summary plot (*bottom left*) showing that in the presence of the FAAH inhibitor URB597 (1 μM) and the CB1R antagonist AM251 (4 μM), AEA (30 μM) depresses MPP- but not MCF-mediated EPSC, an effect that was not associated with changes in PPR and $1/CV^2$ (*right*). **b.** Loading DGCs with AEA (30 μM) also depressed AMPAR-EPSC without changes in PPR and $1/CV^2$. This AEA-mediated depression was blocked by 10 μM CPZ but not 4 μM AM251. **c.** Summary plot (*bottom left*)

and representative traces (*top left*) showing that AEA-mediated depression was abolished in *TRPV1*^{-/-} but not *CBI*^{-/-} mice, and was not associated with PPR or $1/CV^2$ changes (*right*). Number of cells (c) and animals (a) are indicated in parentheses. Summary data consist of mean \pm s.e.m.

Author Manuscript

Author Manuscript

Author Manuscript

Author Manuscript

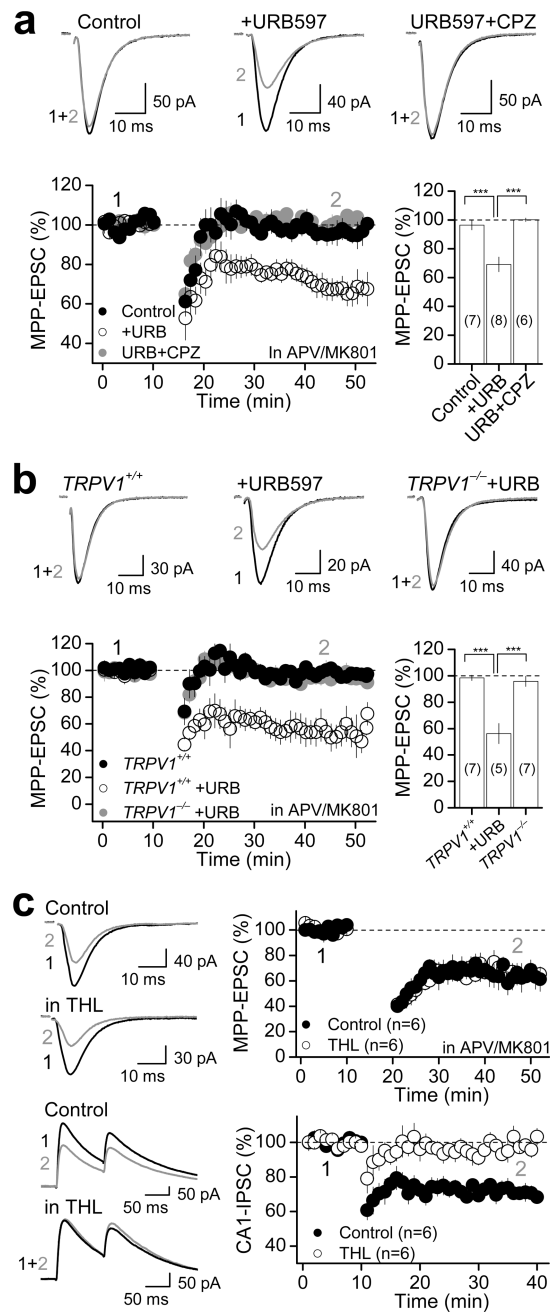


Figure 8. Anandamide mediates TRPV1-LTD in the dentate gyrus

a, Summary plots (*bottom*) and representative traces (*top*) showing that a sub-threshold 1 Hz pairing protocol (4 stimuli -100 Hz- paired with 30 mV depolarization \times 300, rather than \times 600 as seen in previous figures), that triggers no long-term synaptic plasticity under control conditions, triggered robust LTD in the presence of 1 μ M URB597, and this LTD was completely abolished in the presence of 10 μ M CPZ. **b**, A sub-threshold 1 Hz pairing protocol for LTD under control conditions (as seen in rat, panel a) induced robust LTD in the presence of 1 μ M URB597 in *TRPV1*^{+/+} mice (n=3) but not in *TRPV1*^{-/-} mice (n=3). **a**–

b, Number of cells is in parenthesis. *** $p < 0.001$. **c**, Loading DGCs with the diacylglycerol lipase inhibitor THL (4 μM) did not affect the induction of TRPV1-LTD (*top panel*), but abolished the induction of I-LTD in the CA1 area of the hippocampus (*bottom panel*). Averaged EPSCs (*top panel*) and IPSCs (*bottom panel*) before (black) and 25 min after LTD induction (gray) are shown on the left side. Summary plots showing the time course of LTD are shown on the right. Summary data consist of mean \pm s.e.m.